Central European Geology, Vol. 58/3, 199–216 (2015)
DOI: 10.1556/24.58.2015.3.1

Posht-e-Badam Metallogenic Block (Central Iran): A suitable zone for REE mineralization

Mir Ali Asghar Mokhtari*

Department of Geology, Faculty of Science, University of Zanjan, Zanjan, Iran

Received: January 8, 2015; accepted: April 13, 2015

One of the most important ores for REE mineralization are iron oxide–apatite (IOA) deposits. The Posht-e-Badam Block (PBB) is a part of the Central Iranian geostructural zone which is the host of most important Fe deposits of Iran. Exploration studies of the IOA deposits within the PBB (e.g. Esphordi, Gazestan, Zarigan, Lak-e-Siah, Sechahoun, Chahgaz, Mishdovan, Cheshmeh Firouzi and Shekarab) demonstrate that these deposits contain high contents of REE. Concentrations of ∑REE in the most important IOA deposits of the PBB include the following: the Esphordi deposit varies between 1.2 and 1.88%, the Gazestan deposit between 0.17 and 1.57%, the Zarigan deposit between 0.5 and 1.2% and the Lak-e-Siah deposit varies between 0.45 and 1.36%. Concentrations of ∑REE within the apatite crystals present within the IOA ores in the Esphordi, Lak-e-Siah and Homeijan deposits have ranges between 1.9–2.54%, 1.9–2.16% and of 2.55%, respectively. These elements are mainly concentrated in apatite crystals, but other minerals such as monazite, xenotime, bastnasite, urtite, alanite, thorite, parisite–synchysite and britholite have been recognized as hosts of REEs, as small inclusions within the apatite crystals, and in subsequent carbonate, hematite–carbonate and quartz veins and veinlets. Given the extent of this block and the presence of several IOA deposits within this block, and also the high grades of REEs within these deposits, one can reasonably state that it is obvious that there are significant resources of REEs in this part of Iran.

Keywords: Central Iran, iron oxide–apatite (IOA) deposits, Posht-e-Badam Block, REE mineralization, Esphordi, Choghart

* Corresponding address: Boulevard of University, 45371-38791, Zanjan, Iran;
E-mail: amokhtari@znu.ac.ir

ISSN 1788-2281

Introduction

The most important REE ores include peralkaline–alkaline rocks, carbonatites, placers, iron–oxide–copper–gold (IOCG) deposits, iron oxide–apatite (IOA) deposits, pegmatites, vein deposits, skarn deposits and residual deposits (Long et al. 2010). The iron–oxide–copper–gold deposits (IOCG) have been recognized as a distinct deposit type only since the discovery of the giant Olympic Dam deposit in South Australia in the 1980s. The Olympic Dam deposit is unusual in that it contains large amounts of rare earth elements and uranium (Long et al. 2010). Among the iron ores of the world, there is a specific group of occurrences composed of the magnetite–hematite–apatite assemblage (IOA deposits) which are considered as Kiruna-type magnetite–apatite deposits. Rare earth elements (REE) are characteristically elevated in Kiruna-type deposits (Parak 1975; Frietsch and Perdahl 1995; Kerr 1998). REEs tend to partition into apatite, but often provide distinctive accessory mineralogies (Harlov et al. 2002).

The Posht-e-Badam Block (PBB) is a part of Central Iranian geostructural zone. This block is a metallogenic/tectonic province of the Infra-Cambrian age that is host to the most important Fe deposits of Iran between Bafq City to the south and the town of Posht-e-Badam to the north (Figs 1 and 2). Most of these deposits (e.g. Choghart, Chadormalou, Esphordi, Lak-e-Siah, Sechahoun, Cahgaz and Gazestan) are composed of magnetite along with apatite.

Most of the IOA deposits within the PBB were investigated mainly for their mineralogy and genesis; in some cases, it was extended to concentration of REEs within these deposits (Abedian 1983; Darvish Zadeh 1983; Samani and Babakhani 1990;

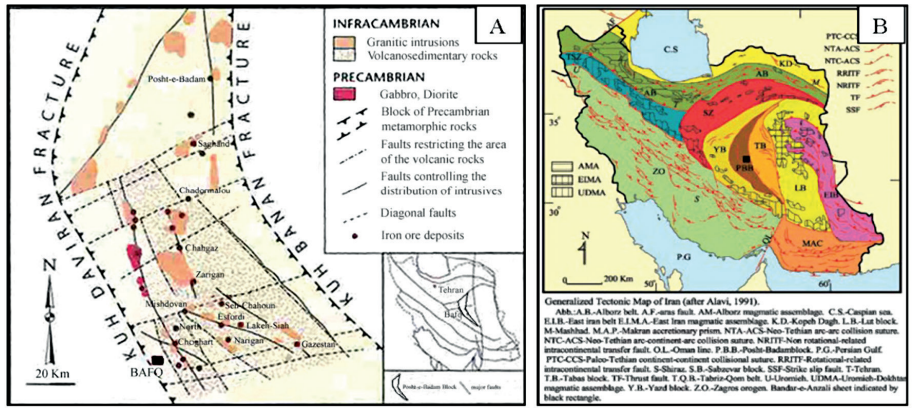

Fig. 1
A: Posht-e-Badam Metallogenic Block, surrounded by the Kuh Banan Fault (to the east) and the Kuh Daviran Fault (to the west). Locations of the most important Fe–P deposits are shown (NISCO 1980). B: Location of the PBB between the Yazd and Tabas Blocks. Locations of the major IOA deposits in this block are indicated by small black squares

Daliran 1990; Forster and Jafar Zadeh 1994; Samani 1998, 1999; Rahmani and Mokhtari 2002; Mokhtari et al. 2003, 2008, 2013).

In this study the results of the REE exploration project within the PBB are presented. This project was carried out by the author as part of the exploration projects of the Geological Survey of Iran.

Fig. 2
Location map of the investigated IOA deposits within the scope of this study on satellite image (Ch: Choghart, Sph: Esphordi, La: Lak-e-Siah, Ga: Gazestan, Ho: Homeijan, Mi: Mishdovan, Ch-F: Cheshmeh Firouzi, S-Ch: Sechahoun, Za: Zarigan, Ch-G: Chahgaz, N-Ch-G: north of Chahgaz, Sh: Shekarab, Chd: Chadormalou)

Research method

This study is in two parts: field work and laboratory investigations. Field work includes sampling from the IOA ores in the PBB for analyzing and determination of REE concentrations. Sampling was carried out based on a rare element exploration project of the Geological Survey of Iran. On this basis, IOA ores of the PBB were considered for sampling. Former studies indicated that the mentioned IOA ores demonstrated high concentrations of REEs. The samples were mainly taken from the P-rich parts of the different IOA ores within the PBB. Sampling was with chip samples in which each sample was about one kilogram in weight. For some IOA ores, apatite crystals were separated for analyzing. In the course of the laboratory work, 57 P-rich IOA ore samples and 8 samples from the apatite crystals were analyzed for REEs and other rare elements by the ICP-MS method (Table 1). These analyses were carried out in the ALS Chemex Laboratory in Canada. The multi-acid digestion method was used to dissolve all minerals, to provide near total values for all elements. The detection limits of the analyzed elements are shown in Table 1.

Geology

The PBB is a metallogenic/tectonic province in the Central Iranian zone (Stöcklin 1968; Alavi 1991; Fig. 1). This block is located between the Yazd Block to the west and the Tabas Block, together with the Lut Block, further to the east. Furthermore, it is bordered by two major fault zones: The Kuh Daviran or Posht-e-Badam Fault to the west and the Kuh Banan Fault to the east (Fig. 1). This zone is a narrow N–S trending

Table 1
Results of analyzed samples from the IOA deposits of the Posht-e-Badam Block in the ALS-Chemex laboratory by ICP-MS method (grads in ppm). Apatite crystals are shown by a star symbol

Sample	Y	Ce	Dy	Er	Eu	Gd	Ho	La	Lu	Nd	Pr	Sm	Tb	Tm	Yb	∑REE
Za.10	502	4770	241	120	22.8	377	38.1	2050	10.7	2640	698	412	45.5	15.3	88.8	12031
Za.12	684	4630	217	114	22.1	333	35.4	2050	10.2	2470	658	368	40.3	14.7	85.2	11732
Za.7	407	3390	162	83.4	15.8	249	25.8	1340	7.47	1670	478	262	30	10.7	62.3	8193.5
Za.9	224	2100	102	53.4	11.6	152	16.5	888	4.76	1010	270	160	18.8	6.94	40	5058
Ga.2	687	5920	354	171	41.1	543	53.7	3120	13.6	3250	857	538	66.7	21.8	121	15758
Ga.7	712	4970	327	160	31	502	49.6	2290	12.1	2810	728	506	59.8	20.4	116	13294
Ga.6	632	5560	307	159	31.1	424	48.7	2720	12.3	2780	748	433	54.2	20.6	114	14044
Ga.4	735	4420	328	171	28.2	454	52.7	2030	14.1	2360	622	422	58.6	22.8	130	11848
Ga.1	245	2290	144	76.4	16.5	213	23.9	1100	6.73	1230	340	216	26.8	9.93	59.2	5997.5
Ga.3	137	1150	60.8	29.8	9.15	98.2	9.4	521	2.5	605	163	105	11.8	3.79	22.3	2928.7
Ga.8	101	634	53.4	30.1	5.6	69.2	8.97	305	2.69	358	93	63.9	9.36	4	24.5	1762.7
Ga.5	98	622	53.2	29	5.75	69.2	8.63	312	2.76	362	92.4	65.6	9.35	3.98	24	1757.9
La.84A*	1383.2	9311	253	138	41.9	498	48.2	4230	10.2	3960	1112	534	56.4	15.2	81	21672.5
La.14*	1019.2	9310	193	106.5	38.2	415	35.8	4230	7.7	3600	1011	437	43.6	11.2	62.3	20520.2
La.11	1087	8410	252	124	35.4	401	39.7	3850	9.47	3690	1070	488	49.2	15.3	85.1	19606
La.13	772	6110	134	74.7	26.2	280	25	2690	5.6	2430	730	301	29.9	8.1	43.5	13660
La.1	743	4420	130	70	18	247	23.8	1905	5.1	1890	540	263	28	7.6	40.9	10330.9
La.108	841	4060	143	81	22.9	236	28.2	1765	6.6	1635	478	251	29.5	9.3	52.8	9639.3

Table 1 (cont.)

Sample	Y	Ce	Dy	Er	Eu	Gd	Ho	La	Lu	Nd	Pr	Sm	Tb	Tm	Yb	∑REE
La.117	916	3580	156	87.9	22.7	231	30.6	1570	7.4	1505	433	242	30.6	10.4	58.6	8880.7
La.100	413	3580	66.1	37.9	13.4	137	12.8	1485	3	1225	391	143	14.9	4	22.4	7548.5
La.9	265	2520	98.4	50.2	12.9	154	15.5	1100	4.29	1150	338	169	18.4	6.43	36.6	5938.7
La.78	238	2150	39.4	21.6	8.2	87.2	7.5	868	1.6	758	238	90.4	9.1	2.3	12.7	4532
Ch.G.3	53	391	5.84	2.2	1.27	14.7	0.74	199	0.24	159	47.8	22.5	1.42	0.27	1.68	900.66
Ch.G.1	92	694	14.4	4.9	3.75	31.7	1.93	314	0.36	282	83.4	40.2	3.28	0.5	3.09	1524.5
Sh.1	53	586	20.8	8.13	4.6	35.8	2.86	258	0.63	219	63.9	38.8	4.13	0.88	5.46	1317
Mi.6	140	405	17.4	6.93	5.52	30.5	2.57	183	0.76	200	51.5	36.1	3.75	0.88	5.6	1089.51
S.Ch.4	140	1050	41.2	20	5.19	61.9	6.98	502	1.67	420	117	66.1	7.75	2.38	13.6	2401.8
Ch.F.3	132	1150	64.7	29.4	8.64	98.3	9.75	559	2.2	524	148	95.1	12.1	3.35	19.7	2856.24
Ch.F.5	110	461	33	13.4	4.7	49.4	4.63	234	0.97	238	64.6	47.5	6.18	1.51	8.87	1277.67
N.Sph.52*	1747.2	11440	296	167	55.6	540	57.5	5200	12.7	4010	1126.4	566	62.9	19.2	105.5	25406
N.Sph.9*	1865.5	10802	295	163.5	54.6	529	60.4	4910	13.6	3890	1092.7	556	62.5	20.5	109.5	24424.8
N.Sph.10*	1401.4	8520	230	128	42	410	46.8	3890	10.6	3150	868	435	49.4	15.4	85.4	19282.8
N.Sph.13	643	3480	112	62.5	21.1	186.5	23	1565	5.4	1325	370	196	23.5	7.8	42.8	8063.6
N.Sph.2	615	2490	101	59.6	14.2	148.5	21	1080	5.5	981	265	149.5	19.4	7.7	41.9	5998.8
N.Sph.55	624	2420	104	59.9	14.8	151.5	20.7	1010	5.2	951	262	152.5	20	7.3	41.2	5851.6
N.Sph.5	492	2220	83.8	47.2	13	129	17.2	940	4.4	878	243	134	17	6.0	33.9	5258.5
N.Sph.15	1192.1	5860	191	106	34.6	318	39	2570	8.8	2230	606	332	39.2	13.1	70.6	13610.4
Sph.60*	1510.6	8210	250	142.5	42.4	430	49	3560	11.4	3140	882	461	62.6	16.6	91.9	18850

Table 1 (cont.)

Sample	Y	Ce	Dy	Er	Eu	Gd	Ho	La	Lu	Nd	Pr	Sm	Tb	Tm	Yb	∑REE
Sph.62*	1528.8	7990	257	144.5	42.9	434	50	3630	11.4	3110	880	462	52.5	16.8	92.5	18704.4
Sph.5	1510	7840	245	118	36.7	357	40.4	3730	10.5	2840	793	412	45.3	14.7	85.2	18078
Sph.4	1125	5950	195	93.8	28.7	283	32.1	2800	8.27	2260	628	334	36.1	11.9	69.8	13856
Sph.63	1073.8	5120	172	101	28.4	288	34.1	2230	8.2	2030	564	297	35.5	11.8	65.9	12059.2
Sph.49	1301.3	5460	209	121	34.3	40.7	40.7	2240	10.2	2300	626	358	42.6	14.3	82.5	13172.9
Sph.57	1183	4470	189	111	27.3	287	37.1	1840	9.2	1950	516	309	37.7	13	72.8	11052.1
Sph.51	1146.6	4390	186	104.5	27.5	287	35.8	1780	8.5	1875	509	307	37.1	12.6	68.7	10775.3
Sph.48	890	3660	147	81.1	23	230	27.9	1485	6.7	1555	425	245	29.6	9.6	53.4	8867.8
Sph.46	993	3300	153	88.5	21	230	30.4	1305	7.6	1475	392	244	30.1	10.8	60.6	8341
Sph.59	936	2730	148	85.5	20.4	198.5	28.9	1145	6.9	1170	319	201	27.7	10.2	56.4	7083.5
Sph.52	548	2040	83.5	51.5	15	122	17	908	5.5	816	228	125	15.8	6.7	41	5023
Sph.45	621	1895	103	58.6	13.2	145	20	759	5.1	879	233	147.5	19.9	7.2	40.4	4946.4
Sph.58	500	1640	81.1	45.8	11.2	120	15.8	657	3.8	736	195	124	16	5.6	31.2	4182.5
Sph.47	71.2	506	11.6	6.5	2.3	22.7	2.2	214	0.5	178	53.7	23	2.6	0.7	4.1	1099.1
Sph.40	1346.8	5250	229	124.5	32.3	363	43.1	2130	10	2330	613	388	46.9	14.8	82.2	13003.6
Sph.41	1255.8	5370	220	119	33.2	371	41.6	2180	9.5	2420	630	390	46.5	13.8	77.1	13177.5
Sph.44	1292.2	5340	227	120.5	33	374	41.8	2160	9.7	2380	629	397	46.8	14.2	78	13143.2
Sph.38	400	1345	62.1	37	7.7	87.2	12.6	565	3.2	563	155.5	89.3	11.8	4.5	25.6	3369.5
Sph.39	385	1335	59.4	35.7	7.6	85.6	12.1	546	3.1	557	153.5	88.8	11.4	4.3	24.2	3308.7
Sph.42	203	753	32.7	192.2	4.6	47.3	6.5	1.7	1.7	311	84.2	48.9	6.4	2.4	13.6	1847.5
Sph.43	224	796	35.8	21.3	4.9	52.6	7.2	1.9	1.9	330	91.6	52.6	7	2.6	14.9	1970.4
Ha.40Ch	327	991	110	53.4	18.8	203	19.4	1370	3.75	1490	378	234	26.7	5.58	27.5	5258.13

Table 1 (cont.)

Sample	Y	Ce	Dy	Er	Eu	Gd	Ho	La	Lu	Nd	Pr	Sm	Tb	Tm	Yb	∑REE
Ha.82Ch	113	612	22.4	10.7	3.65	41.5	4.33	281	1.02	266	72.2	43.5	4.67	1.35	8.01	1485.33
Ha.89Ch	114	611	23.1	10.8	3.79	42.6	4.24	282	1.03	270	73.1	44	4.82	1.37	8.65	1494.5
Ha.94Ch	586	3010	128	57.2	19.5	229	23.7	1320	4.33	1390	354	235	26.8	6.73	33.9	7424.16
Ha.94Ch	275	1830	71.3	29.3	13	134	12	812	2.41	859	233	149	15.4	3.53	20	4458.94
Ha.100Ch	114	522	22.43	11.2	3.73	38.7	4.62	240	1.02	238	63.5	39.9	4.71	1.43	7.29	1312.5
Ha.101Ch	265	1710	58.4	26.1	10.3	114	10.3	769	2.13	749	202	120	12.2	3.04	17.1	4068.57
Ha.103Ch	139	991	31	15.1	5.41	59.8	5.62	426	1.51	407	111	64	6.61	2.18	11.1	2276.33
Ha.23Ch	65.7	698	17.6	7.22	4.43	39.2	2.26	338	0.69	343	94	52.3	4.75	0.82	5.46	1673.43
Ha.26Ch	369	2240	83.2	43.2	13.3	143	15.6	1070	3.39	1060	292	166	20.1	5.1	25.7	5549.59
Ha.27Ch	680	3470	158	86.4	24.2	267	29.7	1900	7.71	2020	523	323	37.8	10.5	52	9589.31
Ha.28Ch	750	3930	176	99.5	24.8	268	33.6	1780	8.68	1980	506	324	40	11.8	60	9992.38
Ha.142Ch	197	1300	43.1	20.4	8.21	86.7	8.16	581	1.74	555	152	88.7	9.07	2.52	13.7	3067.3
Ha.143Ch	214	1460	47.7	21.3	8.51	95	8.61	674	1.94	630	171	99.3	9.91	2.79	16.6	3460.66
Ha.144Ch*	1950	11500	378	196	52.4	679	74.2	4590	17.6	3970	1110	679	76.5	25	129	25426.7
Ha.145Ch	214	1760	53.6	23	9.61	113	9.07	806	1.94	759	206	119	11.8	2.76	16.7	4105.48
Ha.147Ch	553	3710	131	58.1	21.4	252	23.5	1720	4.8	1640	429	262	27.8	7.14	37.3	8877.04
Ha.148Ch	133	1430	36.7	16	8.48	70.4	6.08	533	1.37	575	157	89.3	9.87	1.83	9.55	3076.58
Ha.149Ch	243	1270	56.8	32.8	9.66	90.2	10.7	536	3.87	697	179	126	13.6	4.18	24.8	3297.61
Ha.150Ch	152	945	32.8	17.7	6.06	62	5.99	446	1.5	459	125	71.9	8.26	2.28	11.2	2346.69
Ha.153Ch	323	1560	71.8	40.9	10.1	107	13.6	707	3.84	789	210	132	16.1	4.93	26	4015.27
Ha.111Ch	139	991	31	15.1	5.41	59.8	5.62	426	1.51	407	111	64	6.61	2.18	11.1	2276.33

rift zone (Berberian and King 1981; Samani 1993, Daliran et al. 2009). Rifting took place in the late Precambrian and is characterized by sequences of non-metamorphic volcanic and volcano-sedimentary rocks, dolomitic limestone, local evaporates, bimodal volcanism, large sub-volcanic granitic bodies, syenite, gabbro and later diabasic dykes. Iron-ore deposits, apatite-bearing magmatic rocks which are known as apatitites (Daliran 1999), Pb–Zn ores and Th–U mineralization are related to this riftogenic event (Daliran 1990; Samani 1993). The Early Cambrian magmatism has been attributed to an arc setting by Ramazani and Tucker (2003) whereas the predominantly bimodal volcanism and its alkalic character led Samani (1998), Daliran (2002) and Daliran et al. (2009, 2010) to favor an extensional episode during or shortly after arc magmatism.

The PBB constitutes the most significant Fe-oxide and phosphate deposits in the world. It contains reserves of over 2 billion tons of Fe (NISCO 1980) within more than 34 major magnetic anomalies in a 7,500 km^2 area. Among these targets, 14 have been defined as major deposits with over 1 billion tons of high grade Fe ore (53–65%) (Taghizadeh 1976). The most economic iron ores consist of magnetite with apatite (e.g. at Choghart, Chadormalou, Esphordi, Zarigan, Lak-e-Siah, Gazestan, Sechahoun, Mishdovan, etc.; Figs 1 and 2). SSE–NNW fault lines were important for the tectonic evolution of these ores (Daliran 1990).

The IOA ore bodies of the PBB are hosted by a Lower Cambrian volcano-sedimentary sequence (also known as Saghand Formation) composed of acidic to basic lavas, pyroclastic–epiclastic rocks, intercalated carbonates which are associated with number of mafic and felsic intrusions (Samani 1993; Jami 2005; Torab 2010). Samani (1993) believed that the Saghand Formation was formed between 750 and 550 Ma ago in a riftogenic setting. Volcanic rocks are mainly rhyolitic and rhyodacitic in composition and the sedimentary rocks are mainly dolomite. These ore bodies are commonly associated with pervasively altered acidic–intermediate tuffs. Some IOA ores of this block are associated with green rocks (Daliran 1990; Samani 1993). These rocks are probably the result of alteration in K-feldspars rich intrusions (Daliran 1990). Some researchers (e.g. Samani 1993) called these rocks as metasomatite. In addition to IOA ores, there are several non-ferrous ore bodies containing Pb–Zn (Kushk mine), Mn (abundant Narigan mine) and U (Figs 1 and 2). Pebbles of the iron-oxide ores found in the basal Cambrian conglomerate in the Zarigan area (Haghipour 1975) demonstrate that Fe mineralization occurred during Infra-Cambrian.

REEs mineralization

IOA ores of the PBB are composed of magnetite (±hematite ±martite) and magnetite–apatite. These ores are present in veins, dykes and in massive form within the Lower Cambrian volcano-sedimentary sequence host rocks. In most of these deposits (e.g. Gazestan, Esphordi, Zarigan and Lak-e-Siah), euhedral apatite crys-

tals are present in the magnetite or in the matrix of green rocks with porphyroidic to pegmatoidic texture (Fig. 3). Furthermore, in some deposits (e.g. Esphordi), the concentration of fine-grained apatite crystals formed phosphatic zones within and around the iron ore bodies and green rocks. These deposits were classified as Kiruna-type iron ore deposits (Darvish Zadeh 1983; Daliran 1990; Kryvdik and Mykhaylov 2001; Jami 2005; Torab and Lehman 2008; Torab 2010; Bumeri 2013; Mokhtari et al. 2013).

There are two generations of apatite crystals in the most of these deposits. The first generation includes coarse grained euhedral crystals, and the second generation is made up of fine-grained crystals that are present in the Fe ore matrix. Usually coarse-grained crystals contain inclusions of REE minerals such as monazite, bastnasite, xenotime, and alanite (Kryvdik and Mykhaylov 2001; Jami 2005; Torab and Lehman 2008; Torab 2010; Stosch et al. 2011; Bumeri 2013). Apatite crystals from the PBB are fluorine-rich and rather low in chlorine (Jami 2005; Stosch et al. 2011); this is common for apatite from felsic to intermediate (as well as other) magmatic rocks and independent of their relation to ore systems (Piccoli and Candela 2002).

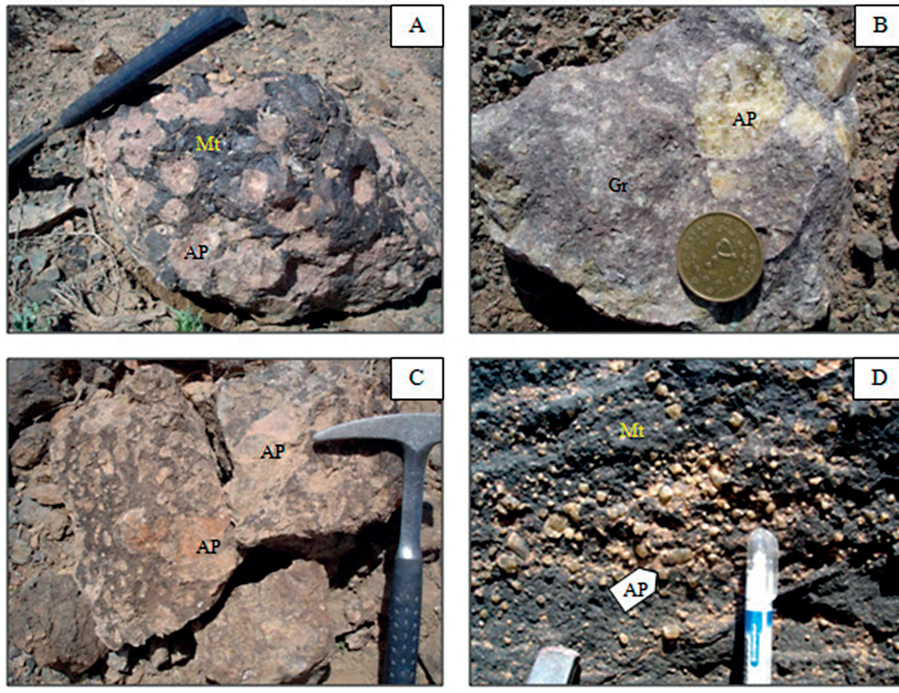

Fig. 3
Euhedral apatite crystals within the magnetite matrix (A: Esphordi deposit, D: Lak-e-Siah deposit) and within the green rocks (B: Esphordi deposit, C: Zarigan phosphate deposit). (Ap: apatite, Mt: magnetite, Gr: green rock)

REE mineralization in the PBB is related to the IOA deposits (Abedian 1983; Darvish Zadeh 1983; Daliran 1990; Samani and Babakhani 1990; Samani 1998, 1999; Kryvdik and Mykhaylov 2001; Rahmani and Mokhtari 2002; Jami 2005; Mokhtari and Emami 2008; Torab and Lehman 2008; Torab 2010; Bumeri 2013; Mokhtari et al. 2013). In fact, enrichment in REEs is one of the specific characteristics of the IOA ores in this region. These elements are mainly concentrated in apatite crystals, but other minerals such as monazite, xenotime, bastnasite, urtite, alanite, thorite, parisite–synchysite and britholite, which are enriched in REEs, have been recognized (Kryvdik and Mykhaylov 2001; Jami 2005; Torab and Lehman 2008; Torab 2010; Bumeri 2013). These minerals are present as small inclusions within the apatite crystals, as well as in subsequently-emplaced carbonate, hematite–carbonate and quartz veins and veinlets (Kryvdik and Mykhaylov 2001; Jami 2005; Torab 2010; Bumeri 2013). Previous studies indicate that some of these inclusions were formed as primary deposits (Kryvdik and Mykhaylov 2001), but most of them were generated as secondary one as a result of later percolation of hydrothermal fluids (Jami 2005; Torab 2010; Bumeri 2013).

Geochemical investigations demonstrate that REE concentrations have a good positive correlation with P_2O_5 contents and negative correlation with Fe content (Mohamadi 2014). This is in turn indicative of REE concentrations within apatite and other phosphate minerals (e.g. monazite, xenotime and bastenasite).

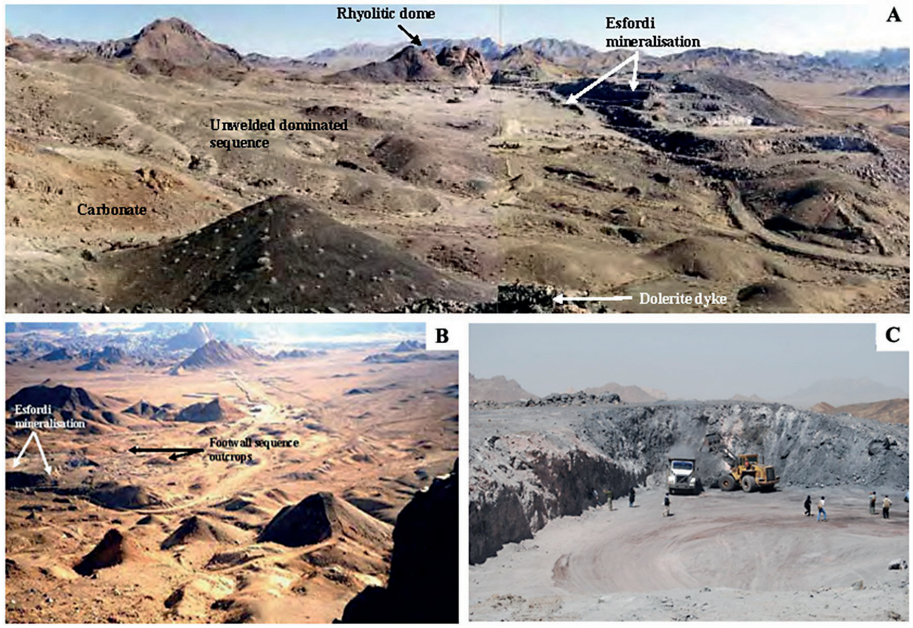

Fig. 4
Some views from the Esphordi P–Fe deposit. A: View to the SE, B: View to the S, C: Views from the exploitation site in the Esphordi P–Fe deposit (view to the SE). Figures A and B taken from Jami (2005)

Esphordi IOA deposit

The Esphordi IOA deposit is hosted by a Cambrian-age sequence of volcano-sedimentary rocks (Jami 2005). This area is composed of rhyolite and rhyolitic tuff, dolomite, sandstone, altered volcano-sedimentary rocks, diabasic dykes and IOA ores (Jami 2005; Fig. 4). In this deposit, there is a main phosphatic zone which is mined for this purpose, and is called the Esphordi Phosphate deposit. Some previous investigations of the Esphordi deposit (Abedian 1983; Darvish Zadeh 1983; Samani and Babakhani 1990; Samani 1998, 1999; Daliran 1990; Kryvdik and Mykhaylov 2001; Jami 2005; Mokhtari and Emami 2008; Torab 2010) have demonstrated remarkable concentrations of REEs. There are inclusions of titanite, monazite, bastnasite, xenotime, britholite, parisite–synchysite, urtite and alanite within the apatite crystals, in which their concentration reach up to 2% (Kryvdik and Mykhaylov 2001; Jami 2005;

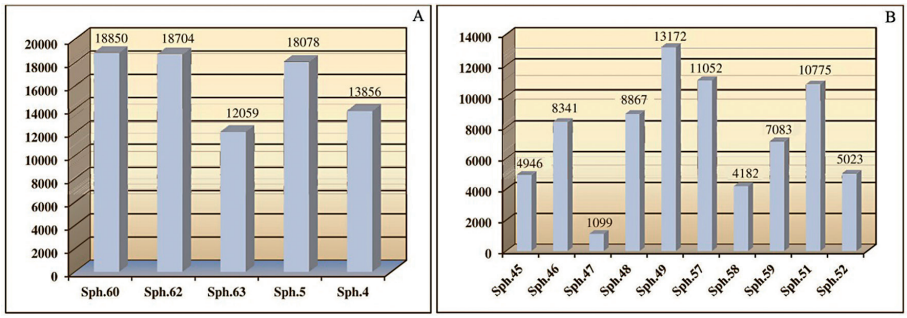

Fig. 5
A: REE concentrations in the samples from the Esphordi P–Fe deposit. B: REE concentrations in the samples from the IOA ores in the west of the Esphordi deposit (grades in ppm)

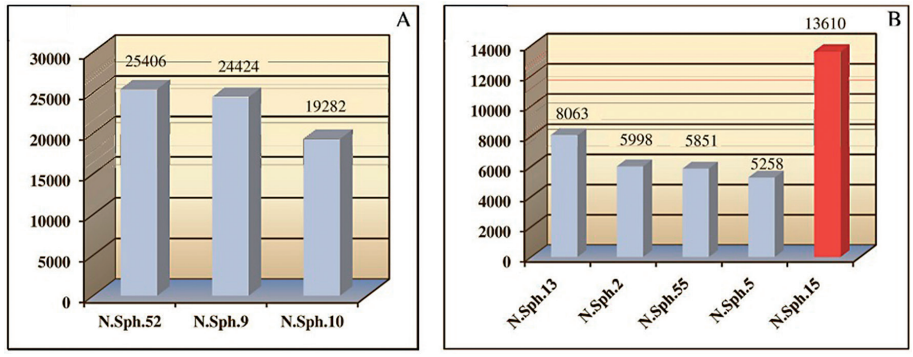

Fig. 6
A: REE concentrations in the samples from the apatite crystals from the IOA ores in the north of the Esphordi deposit. B: REE concentrations in the samples from the apatite-bearing magnetite ores and pyrite and hematite-bearing silica vein from the north of the Esphordi deposit (grades in ppm)

Torab 2010, Bumeri 2013). REE content is directly related to the concentration of these inclusions (Kryvdik and Mykhaylov 2001; Jami 2005; Torab et al. 2008; Torab 2010).

Analysis of the samples from the Esphordi IOA deposit during this study indicates a higher grade of REEs, which varies between 1.2 and 1.9% (Fig. 5). Furthermore, there are some small outcrops of IOA ores in the western part of the Esphordi deposit. REE content in these ores varies between 0.11 and 1.3% (Fig. 5). Lower grades belong to magnetite ores with negligible amounts of apatite. There are also some other small IOA ores that crops out to the north of the Esphordi deposit. The REE content in the apatite-bearing magnetite ores is between 0.5 and 0.8% (Fig. 8). Samples from the apatite crystals of these ores demonstrate higher grades of REEs between 1.9 and 2.5% (Fig. 6). One sample from the younger pyrite and hematite-bearing silica vein (N.Sph.15) indicates a high content of REEs (1.36%), which is enriched in HREEs (Fig. 6).

Gazestan IOA deposit

This deposit is composed of Upper Proterozoic to Cambrian green rocks that are surrounded by dolomite, shale and sandstone, along with intercalations of acidic lavas and tuffs and cherty layers of the same age (Fig. 7). Phosphate mineralization in this

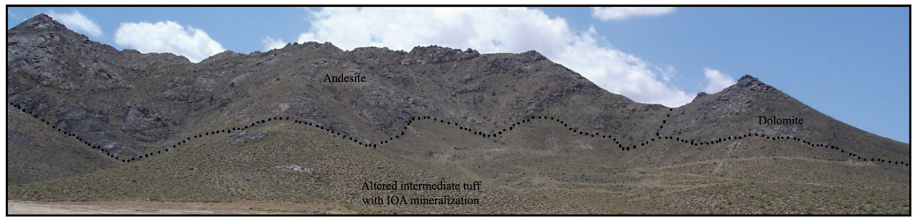

Fig. 7
A view from the Gazestan IOA deposit (view to the SW)

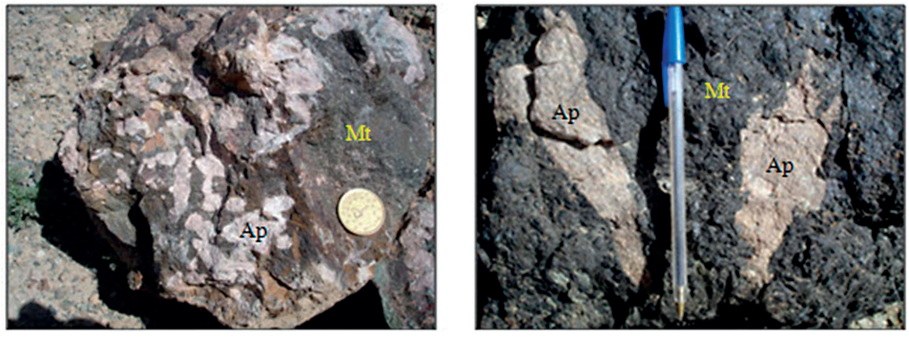

Fig. 8
Coarse-grained euhedral apatite crystals in the magnetite matrix at the Gazestan IOA deposit (Ap: apatite, Mt: magnetite)

area is present as coarse-grained apatite crystals in the magnetite matrix (Fig. 8), phosphatic veins with minor accompaniment of magnetite and veinlets of fine-grained apatite crystals within the green rocks. IOA ores are present as small lenses and veins within the altered green rocks. Based on Kryvdik and Mykhaylov (2001), mineralization in the Gazestan IOA deposit is poly-stage, where the first stage was one of magnetite–apatite mineralization and the later stage led to the formation of the major phosphatic zone.

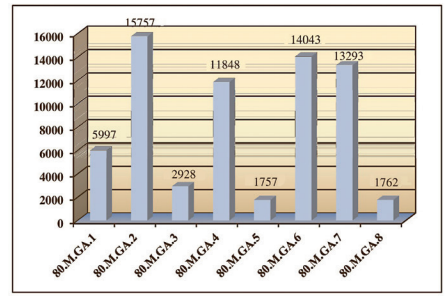

Fig. 9
REE concentrations in the samples from the Gazestan IOA deposit (grades in ppm)

Kryvdik and Mykhaylov (2001) reported that the REE content in the Gazestan IOA deposit is about 1.5%. The results of sample analysis in this study demonstrate that REE grades are between 0.17 and 1.57 percent (Fig. 9), being directly related to the P_2O_5 content.

Zarigan phosphate deposit

This area is made up of Upper Proterozoic–Cambrian rhyolite, syenite, granites and altered green rocks cut by diabasic dykes (Fig. 10). These altered rocks contain diopside, apatite, tremolite–actinolite and some calcite and quartz. Unlike the other IOA deposits of the PBB, this deposit includes only some phosphatic veins (up to 1 m in thickness) that are coarse-grained and of pegmatoidic texture (Fig. 11); iron oxide mineralization is absent in this deposit. The phosphatic veins show a NE–SW trend.

Previous studies (Abedian 1983; Kryvdik and Mykhaylov 2001) indicated high grades of some REEs (involved La, Ce, Pr and Nd) within the apatite crystals of this deposit (more than 1% for these 4 mentioned elements). The results of our studies demonstrate that the REE content in the whole rock samples from this deposit varies between 0.5 and 1.2% (Fig. 12).

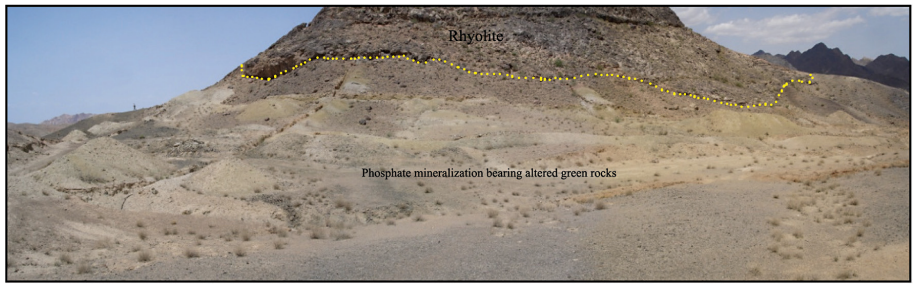

Fig. 10
A view from the Zarigan phosphate deposit in the hillside of rhyolite (view to the N)

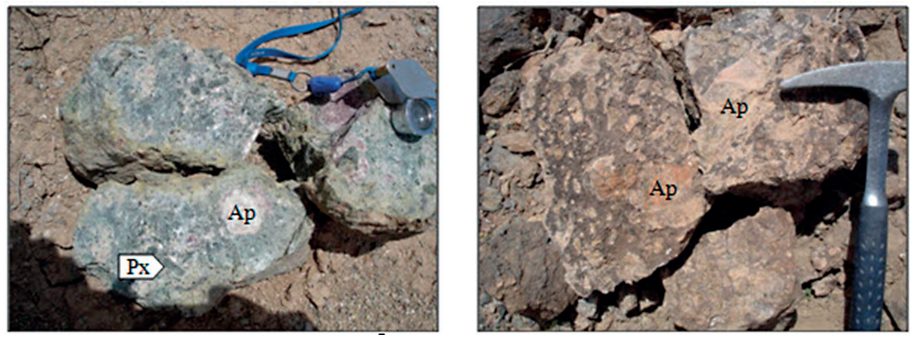

Fig. 11
Coarse-grained euhedral apatite within the green rocks at the Zarigan phosphate deposit (Ap: apatite, Px: pyroxene)

Lak-e-Siah IOA deposit

This area consists of rhyolite and rhyolitic tuffs, intermediate tuffs and some dolomite. Small outcrops of syenitic and gabbroic intrusion are also present (Fig. 13). There are some green rocks (tremolite–actinolite–apatite) in some places. IOA ores can be seen as lenses and veins in this area. Mineralogically, they are composed of magnetite that underwent martitization. Phosphate mineralization

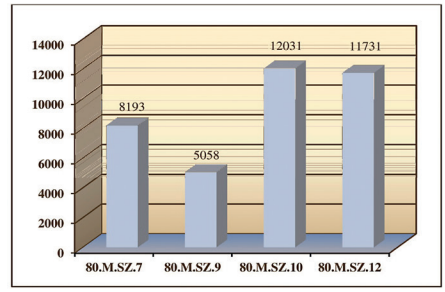

Fig. 12
REE concentrations in the samples from the Zarigan Phosphate deposit (grades in ppm)

Fig. 13
View from the exploited Lak-e-Siah IOA apatite deposit (view to the SW)

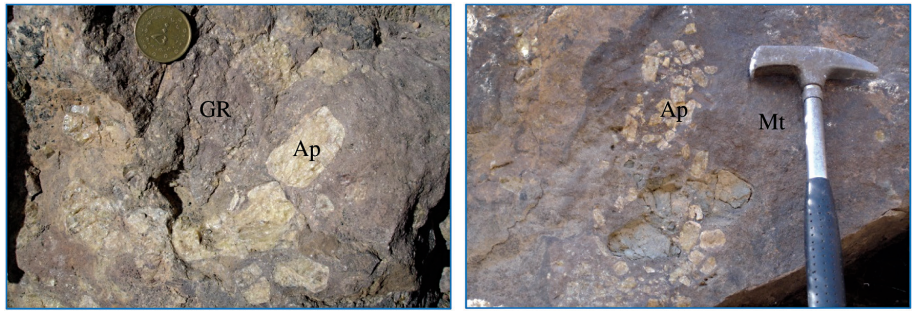

Fig. 14
Euhedral apatite crystals within the magnetite and green rocks at the Lak-e-Siah IOA deposit (Ap: apatite, Mt: magnetite, GR: green rock)

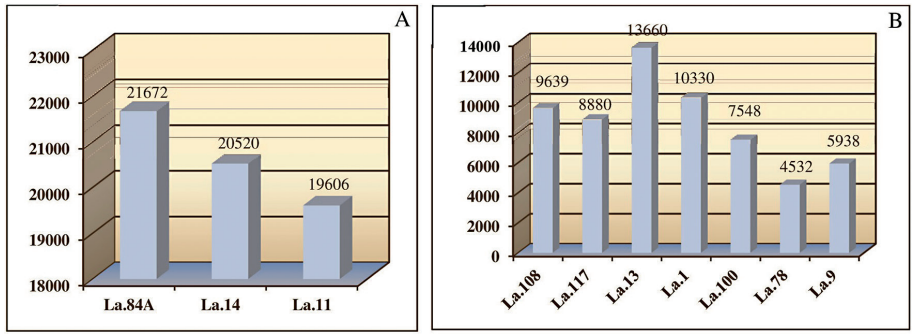

Fig. 15
A: REE concentrations in the apatite crystals within the IOA ores in the Lak-e-Siah deposit. B: REE concentrations in the samples from the apatite-bearing magnetite ores of Lak-e-Siah deposit (grades in ppm)

is present as veins and disseminated apatite crystals within the iron ores and green rocks (Fig. 14).

The analysis results of the samples from the apatite crystals demonstrate that the REE content varies between 1.96 and 2.16% (Fig. 15). In the samples from the apatite-bearing Fe ores, the REE content varies between 0.45 and 1.36% (Fig. 15).

Other IOA deposits of the Posht-e-Badam Block

The IOA deposits of Sechahoun, Mishdovan, Chahgaz, north of Chahgaz, Cheshmeh Firouzi, Shekarab and Homeijan also indicate high grades of REEs. Geologically and lithologically, these deposits are the same as the previously-mentioned IOA apatite deposits. Magnetite is the main form of mineralization in these deposits, which is martitized in some places. Phosphate mineralization is present as veins, veinlets and disseminated euhedral apatite crystals within or around the Fe ores.

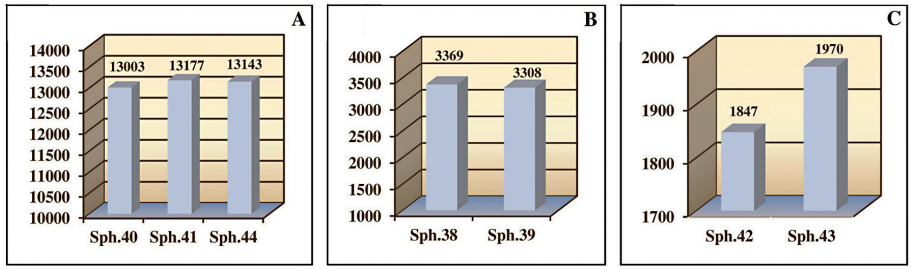

Fig. 16
REE concentrations in the phosphate concentrate (A), waste (B) and Fe concentrate in the Esphordi mine (grades in ppm)

Sample analyses from these deposits demonstrate somewhat high concentrations of REEs. Their REE contents are as follow: 0.24% in Sechahoun, 0.11% in Mishdovan, 0.09–0.15% in Chahgaz, 0.08–0.14% in NE Chahgaz, 0.13–0.28% in Cheshmeh Firouzi, 0.13% in Shekarab and 0.13–1% in the Homeijan deposit. Apatite crystals from the Homeijan IOA deposit indicate a 2.55% REE content.

Esphordi mine products

As mentioned in the previous sections, phosphatic and IOA ores from the Esphordi deposit have high contents of REEs. Thus it was decided to evaluate the REE concentration in the phosphate concentrate, Fe concentrate and waste of the Esphordi mine. These studies led to a remarkable result. Analyses of the samples from the phosphate concentration demonstrate that the REE content is about 1.3%, samples from the Fe concentrate indicate 0.18 to 0.19% REE content and samples from the waste have 0.33% REE concentrations (Fig. 16).

Conclusions

The IOA deposits of the PBB are enriched in REEs. Among these deposits, the Esphordi, Zarigan, Gazestan and Lak-e-Siah deposits are the most important ones for REE mineralization and recommended for future exploration programs.

Given the high content of REEs in the phosphate concentrate in the Esphordi mine, in view of the higher economic value (price) of these elements, the processing of REEs in this mine and other IOA deposits of the PBB must be taken into consideration.

Finally, it must be remembered that the Posht-e-Badam Metallogenic Block is a valuable zone for REE mineralization, and must therefore be considered as a mining asset. These elements are of considerable economic and technical value; ignoring the concentration of REEs in these deposits would be wasting a national treasure.

Acknowledgements

This research is mainly the result of a rare element exploration project by the Geological Survey of Iran. Therefore, I would like to thank Eng. Korehi, the Head of the Geological Survey of Iran, Dr. Mehrpartou, the Exploration Assistant, and Eng. Abedian, the Manager of the Exploration Branch of Geological Survey of Iran, for their help in analyzing samples in the ALS-Chemex Laboratory.

References

Abedian, N. 1983: Detailed exploration on Esphordi phosphate deposit. – Geological Survey of Iran, Tehran, 68 p. (in Persian)

Alavi, M. 1991: Tectonic map of the Middle East. – Geological Survey of Iran, Tehran.

Berberian, M., G.C.P. King 1981: Towards a paleogeography and tectonic evolution of Iran. – Canadian Journal of Earth Science, 18, pp. 210–265.

Bumeri, M. 2013: Rare earth minerals in Esphordi magnetite-apatite ore deposit, Bafq district. – Scientific Quarterly Journal, Geosciences, 22/85, pp. 71–82. (in Persian)

Daliran, F. 1990: The magnetite-apatite deposit of Mishdovan, east central Iran. An alkali rhyolite hosted Kiruna-type occurrence in the infra Cambrian Bafq metallotect. – PhD thesis, Univ. of Heidelberg, Geowiss. Abhandl., 37, 248 p.

Daliran, F. 1999: REE geochemistry of Bafq apatites: Implication for the genesis of Kiruna-type iron ores. – In: Stanley, C.J. et al. (Eds): Mineral Deposits: Processes to Processing. Balkema, Rotterdam, pp. 631–634.

Daliran, F. 2002: Kiruna-type iron oxide-apatite ores and apatitites of Bafq district, Iran, with an emphasis on the REE geochemistry of their apatites. – In: Porter, T.M. (Ed): Hydrothermal Iron Oxide Copper-Gold and Related Deposits. PGC Publishing, Linden Park, pp. 303–320.

Daliran, F., H.G. Stosch, P. Williams 2009: A review of the Early Cambrian Magmatic and Metasomatic events and their bearing on the genesis of the Fe oxide-REE-apatite deposits (IOA) of the Bafq District, Iran. – In: William, P.J. et al. (Eds): Smart Science for Exploration and Mining: Proceedings of the 10th Biennial SGA Meeting, Townsville, pp. 623–625.

Daliran, F., H.G. Stosch, P. Williams, H. Jamali, M.B. Dorri 2010: Early Cambrian Iron Oxide-Apatite-REE (U) Deposits of the Bafq District, East-Central Iran. – In: Corriveau, L., H. Mumin (Eds): Exploring for Iron Oxide Copper-Gold Deposits: Canada and Global Analogues. Geol. Assoc. Canada, Short Course Notes, 20, pp. 143–155.

Darvish Zadeh, A. 1983: Investigation of the phosphate in Bafq (Esphordi). – Journal of Science, University of Tehran, 28/1, pp. 2–24. (in Persian)

Forster, H.A., Jafar Zadeh 1994: The Bafq mining district in central Iran – a high mineralized infra Cambrian volcanic field. – Economic Geology, 89/8, pp. 1697–1721.

Frietsch, R., J.A. Perdahl 1995: Rare earth elements in apatite and magnetite in Kiruna-type iron ores and some other iron ore types. – Ore Geology, 9, pp. 489–510.

Haghipour, A. 1975: Etude geologique de la region de Biabanak–Bafq (Iran central): petrography et tectonique du scale Precambrian et de sa couverture. – PhD thesis, Grenoble University, 403 p.

Harlov, D.E., H.J. Forster, T.G. Nijland 2002: Fluid-induced nucleation of (Y+REE)-phosphate minerals within apatite: Nature and experiment. Part 1: Chlorapatite. – American Mineralogist, 87, pp. 245–261.

Jami, M. 2005: Geology, geochemistry and evolution of the Esphordi phosphate-iron deposit, Bafq area, Central Iran. – Unpublished PhD thesis, 403 p.

Kerr, I.D. 1998: Mineralogy, chemistry and hydrothermal evolution of the Pea Ridge Fe-oxide-REE deposit, Missouri, USA. – Unpublished MSc thesis, University Windsor, Ontario, 112 p.

Kryvdik, S., V. Mykhaylov 2001: The potential of the rare earth mineralization of Islamic republic Iran. – National Academy of Science of Ukraine, Kiev, 48 p.

Long, K.R., B.S. Van Gosen, N.K. Foley, D. Cordier 2010: The Principal Rare Earth Elements Deposits of the United States; A Summary of Domestic Deposits and a Global Perspective: USGS. Scientific Investigations Report, 2010–5220. – http://pubs.usgs.gov/sir/2010/5220, 96 p.

Mohamadi, F. 2014: Geochemistry of Azim-Abad granitoid (SW of Bahabad) and its probable role in iron-apatite mineralization. – Unpublished MSc thesis, University of Zanjan. (in Persian).

Mokhtari, M.A.A., M.H. Emami, Sh. Rahmani 2003: REE mineralization in the Bafq-Posht-e-Badam region. – 22th Geoscience Symposium, Geological Survey of Iran. (in Persian)

Mokhtari, M.A.A., M.H. Emami 2008: REE pattern and REE mineralization in apatite–magnetite deposits of Bafq-Saghand district (Central Iran). – Geosciences, Scientific Quarterly Journal, Special Issue, 17/1, pp. 162–169.

Mokhtari, M.A.A., Gh. Hossein Zadeh, M.H. Emami 2013: Genesis of iron-apatite ores in Posht-e-Badam Block (Central Iran) using REE geochemistry. – Journal of Earth System Sciences, 122/3, pp. 795–807.

NISCO 1980: Result of search and valuation works at magnetic anomalies of the Bafq iron ore region during 1976–1979. – Unpublished Report, National Iranian Steel Corporation, 260 p. (in Persian)

Parak, T. 1975: Kiruna iron ores are not intrusive magmatic ores of the Kiruna-type. – Economic Geology, 70, pp. 1242–1258.

Piccoli, P.M., P.A. Candela 2002: Apatite in igneous systems. – In: Kohn, M.J., J. Rakovan, J.M. Hughes (Eds): Phosphates (Reviews in Mineralogy and Geochemistry). Mineralogical Society of America and Geochemical Society, Washington, 48, pp. 255–292.

Rahmani, Sh., M.A.A. Mokhtari 2002: Exploration of metallic rare elements. – Geological Survey of Iran, Tehran, 365 p. (in Persian)

Ramazani, J., R.D. Tucker 2003: The Saghand region, Central Iran: U-Pb geochronology, petrogenesis and implications for Gondwana tectonics. – American Journal Science, 303, pp. 622–665.

Samani, B. 1993: Saghand formation, a riftogenic unit of upper Precambrian in central Iran. – Geosciences, Geological Survey of Iran, 6, pp. 32–45. (in Persian)

Samani, B. 1998: Precambrian metallogeny in Central Iran. – Scientific Bulletin of the Atomic Energy Organization of Iran, 17, pp. 1–16. (in Persian)

Samani, B. 1999: Rare earth element mineralization in Precambrian of Central Iran. – Scientific Bulletin of the Atomic Energy Organization of Iran, 20, pp. 15–31. (in Persian)

Samani, B., A. Babakhani 1990: Geological evolution of the Bafq-Saghand region and metallogenic model for the iron-apatite and radioactive deposits. – 9th Symposium on Geosciences, pp. 24–25. (in Persian)

Stosch, H.G., R.L. Romer, F. Daliran, D. Rhede 2011: Uranium-lead ages apatite from iron oxide ores of the Bafq District, East-Central Iran. – Mineralium Deposita, 46, pp. 9–21.

Stöcklin, J. 1968: Structural history and tectonics of Iran: A review. – American Association of Petrology and Geology Bulletin, 52, pp. 1229–1258.

Taghizadeh, N. 1976: The iron ore deposits of Iran. – In: Zitzmann, A. (Ed): The Iron Ore Deposit of Europe and Adjacent Areas; Explanatory Notes to the International Map of the Ion Ore Deposits of Europe. Bundesanstalt fur Geowissenschaften und Rohstoffe, Hannover, pp. 199–202.

Torab, F.M. 2010: Geochemistry and radio-isotope studies on the iron-apatite ores in Bafq metallogenic zone for determination of apatite origin. – Iranian Journal of Crystallography and Mineralogy, 18/3, pp. 409–418. (in Persian)

Torab F.M., B. Lehmann 2008: Magnetite-apatite deposits of the Bafq district, Central Iran: apatite geochemistry and monazite geochronology. – Mineralogical Magazine, 71, pp. 347–363.